


CARBON STORAGE IN HUNAN PROVINCE: MONITORING, MODELING, AND MANAGEMENT STRATEGIES FOR CLIMATE CHANGE MITIGATION

Seyed Omid Reza Shobairi ^{1,2} , Sun Lingxiao ^{1,2}, Zhang Haiyan ^{1,2}, Li Chunlan ^{1,2}, He Jing ^{1,2}, Behnam Asghari Beirami ³, Samira Hemmati Roudbari ⁴, Hadis Sadeghi ⁵, Mohsen Shariati ⁶, Mehran Alizadeh Pirbasti ⁷

¹ Xinjiang Institute of Ecology and Geography, Chinese Academy of Sciences, Urumqi, China

² University of Chinese Academy of Sciences, Beijing, 100049, China

³ Department of Photogrammetry and Remote Sensing, K. N. Toosi University of Technology, Tehran, Iran

⁴ Department of Soil Science, Faculty of Agriculture, University of Zanjan, Iran

⁵ Physical Geography Department, Faculty of Geography, University of Tehran, Tehran, Iran

⁶ Department of Environment Science, University of Tehran, Iran

⁷ Department of Remote Sensing, Hekmat Institute of Higher Education, Qom, Iran

KEY WORDS: Carbon Storage, Monitoring, Modelling, Remotely Sensed Data, Hunan Province

ABSTRACT: Climate change caused by human emissions of greenhouse gases, especially carbon dioxide (CO₂), is one of the most important environmental challenges that the world is facing today. Understanding the spatial and temporal dynamics of CO₂ emissions is critical to inform effective mitigation strategies. This study investigated the carbon emission profile of Hunan Province, an important industrial and economic region in southern China. Using remote sensing technology, spatial statistical techniques, and time series modelling, the researchers identified high-risk and low-risk carbon emission clusters in Hunan Province. In addition, the study examined the key socio-economic and energy-related factors that drive CO₂ output. Finally, the authors developed a forecasting model to predict the trace of carbon emissions over the next decade. The results demonstrate the power of integrating statistical methods and geographic forecasting to provide evidence-based insights to support carbon management policies at the province level. This multifaceted methodology can be replicated in other regions to strengthen greenhouse gas monitoring and emission reduction planning at domestic scales. These findings underscore the critical role of China's provinces in addressing the global climate crisis through targeted data-driven mitigation efforts.

1. INTRODUCTION

CO₂ emissions that cause climate change are mostly generated from the large-scale utilization of fossil fuels. Southeast Asian countries, i.e., Japan, South Korea, China, etc.,

have seen a continuous increase in CO₂ emissions and the growing impact of global warming in the past decades (Nguyen, 2019). For example, the growth in global carbon emissions from burning fossil fuels and cement production occurred in China between 2010 and 2012 (Liu et al., 2015). In 2013, China emitted 25% of all global CO₂ (Liu et al., 2015; Mi et al., 2017). As China is one of the global sources of CO₂ emissions, its carbon emissions need to be accurately quantified (Liu et al., 2013; Wang et al., 2012; Wang and Cai, 2017), to prioritize climate change mitigation. China pledged in its 2015 proposed nationally determined contributions to reduce its CO₂ emissions per GDP unit by 60–65% (compared to 2005 levels) by 2030 (Xinhua, 2015). Despite slowing economic activity and changing economic structure, China has remained the world's largest energy consumer, accounting for 23% of global energy consumption (The British Petroleum (BP) Company, 2016). Rapid growth in the gross domestic product since the 1980s has made China the fourth-largest economy and the third-largest exporter in the world as of mid-2006 (World Trade Organization, 2007). This economic growth is also seen in Hunan province, which is one of the largest economic and energy-consuming provinces in southern China. In late 2010 Hunan was designated as one of the 13 pilot low-carbon zones in China by the National Development and Reform Commission (NDRC) to explore the pathway of low-carbon development. In the context of the new round of economic development, Hunan is seeking a low-carbon economic transition. Hunan has four main pathways to developing low low-carbon economy: energy saving and efficiency improvement, development of low-carbon energy (such as renewable energy, nuclear, and natural gas), forestry and carbon offsetting, and Carbon Capture and Storage (CCS). However, this region is also under pressure to protect its environment, keep its development sustainable, and reduce carbon emissions. Therefore, accurate geospatial statistics and analysis of CO₂ emissions and analyzing the factors influencing these emissions are vital. Hence, the subject better captures the key focus areas of the research:

- Spatial and temporal patterns of CO₂ emissions;
- Identification of high-risk and low-risk emissions clusters;
- Factors influencing the spatial distribution of emissions;
- Forecasting future CO₂ emission trends.

The subject concisely conveys the integrated, data-driven approach used in the study to examine carbon dynamics at the provincial scale in China. It highlights the policy-relevant insights the research aims to provide for supporting carbon mitigation efforts.

2. MATERIALS AND METHODS

2.1. Study area and dataset

Hunan Province is located in the southern part of China (Figure 1). Its coordinates are approximately 27.6° N and 111.8° E. Hunan Province is bounded by several provinces in China. To the north, it is bordered by Hubei Province; to the west, it is bordered by Guizhou Province; to the south, it is bordered by Guangdong and Guangxi Provinces; and to the east, it is bordered by Jiangxi Province. The capital of Hunan is Changsha city.

According to the National Bureau of Statistics of China, as of 2020, the population of Hunan Province was approximately 69.2 million people. The annual population growth rate for Hunan Province from 2010 to 2020 was about 0.48%. According to the National Bureau of Statistics of China, Hunan's Gross Regional Product (GRP) in 2020 was approximately 4.38 trillion yuan (about 674 billion USD), representing a growth rate of 3.5% compared to the previous year. According to the National Bureau of Statistics of China, as of 2020, the total cultivated land area in Hunan Province was approximately 6.88 million hectares. According to the State Forestry and Grassland Administration of China, as of 2020, the forest coverage rate in Hunan Province was 59.85%, with a total forest area of approximately 16.96 million hectares. As for wildfires, Hunan Province has experienced occasional wildfire incidents in recent years, particularly during dry and hot seasons. According to the local authorities, in 2020, there were a total of 28 wildfires in Hunan Province, which burned about 151 hectares of forest land.

In fact, the relationship between forest fires and carbon dioxide (CO₂) production is an important topic in the context of climate change and the global carbon cycle. Here are some key points about this relationship:

1. Carbon storage in forests; Forests act as a major carbon sink, storing large amounts of carbon in their biomass (trees, vegetation) and soil.
2. Carbon release during fires; When forests experience wildfires or are intentionally burned, the stored carbon is released back into the atmosphere as CO₂ and other greenhouse gases. Larger, more intense fires can release significant amounts of CO₂ into the atmosphere, contributing to the overall global CO₂ budget.
3. Impacts on the carbon cycle; Forest fires disrupt the natural carbon cycle, as the carbon stored in the forest is rapidly released instead of being slowly released through natural decomposition. The increased CO₂ levels in the atmosphere can then lead to further climate change, which can, in turn, increase the risk of future forest fires, creating a feedback loop ([Metsaranta et al., 2023](#); [Flannigan et al., 2005](#)).

The local authorities have been taking measures to prevent and control wildfires in Hunan province, such as increasing patrol and monitoring, establishing fire prevention zones, and promoting public awareness of fire safety.

According to the National Bureau of Statistics of China, in 2020, Hunan Province's CO₂ emissions were approximately 361 million tons. This represents an increase of about 2.1% from the previous year. Hunan Province has been taking steps to reduce its carbon footprint and promote sustainable development. The province has set targets to peak its carbon emissions by around 2025 and achieve carbon neutrality by around 2060. To achieve these goals, Hunan Province is promoting the use of clean energy, enhancing energy efficiency, and implementing low-carbon policies and technologies across various sectors, such as transportation, industry, and construction. According to the National Bureau of Statistics of China, in 2020, Hunan Province's CO₂ emissions by sector were as follows: 1) Industry: 214 million tons (59.3%), 2) Transportation: 69 million tons (19.1%),

3) Residential and commercial sectors: 36 million tons (9.9%), 4) Agriculture, forestry, and fishing: 26 million tons (7.3%), 5) Others: 16 million tons (4.4%).

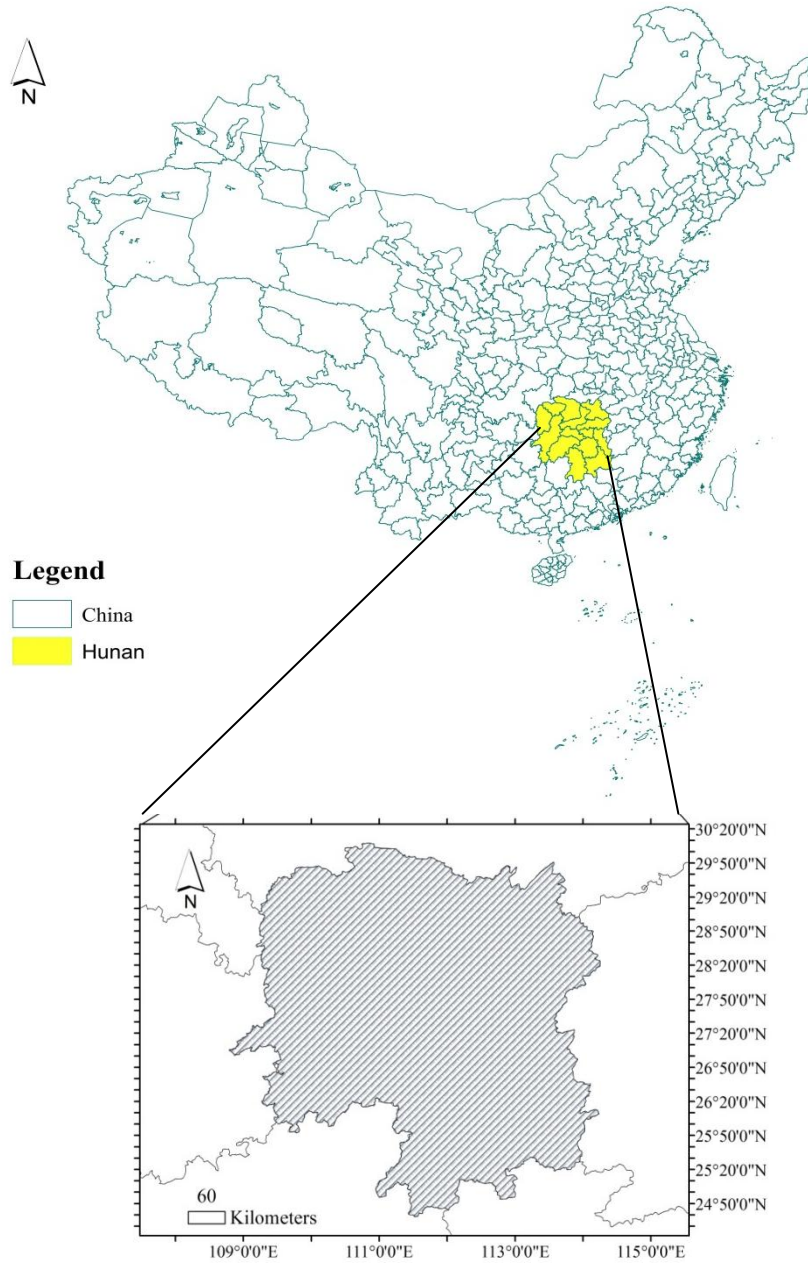


Figure 1. The geographical area of Hunan province

As can be seen from these figures, the industrial sector is the largest contributor to CO₂ emissions in Hunan Province, followed by the transportation sector. The residential and commercial sectors are also significant contributors, although to a lesser extent. In this study, various methods have been employed in order to conduct a spatial analysis of Carbon Storage (CS). CO₂ emission data is extracted for 1990-2021 from Giovanni (<https://giovanni.gsfc.nasa.gov/giovanni/database>) and other databases ([ISLSCP II Globalview: Atmospheric CO2 Concentrations \(nasa.gov\)](#)). We also used the Earth data site (<https://earthdata.nasa.gov>) from 2000 to 2021 and the Giovanni site (<https://giovanni.gsfc>) to collect carbon dioxide data from 1990 to 2000. The accuracy of the data taken from the AIRS/Aqua L3 satellite is 2.5 degrees x 2 degrees. The data is a geometric structure of a raster with a geographical coordinate system. One of the advantages of this data is that it is ready and does not need to be corrected or pre-processed, and for this study on this scale, the data are very suitable (Table 1).

Table 1. The carbon dioxide (CO₂) data product

Variable	Units	Source	Temp.Res	Spat.Res (degrees)	Begin date	End date
CO ₂	ppm	AIRS	Monthly	2*2.5	2000	2020- ongoing
		Global/ NOAA CMDL				
CO ₂	ppm	cooperative air sampling network	Monthly	2*2.5	1990	2000

The annual spatial and temporal trend of the CS changes in the study zone has been evaluated. Thus, using the OLS, SLM, SEM, MGWR, and GWR regressions, spatial modeling of the CS has been explored in ArcGIS besides considering its influential factors such as LST, NDVI, and Land use. High and low-risk spots of the CS were examined through spatial autocorrelation, Average Nearest Neighbor, Kernel Density, Hot spot, and Cluster and Outlier analysis before spatial modeling of dependent and independent variables. Figure 2 summarizes the stages of the present study generally.

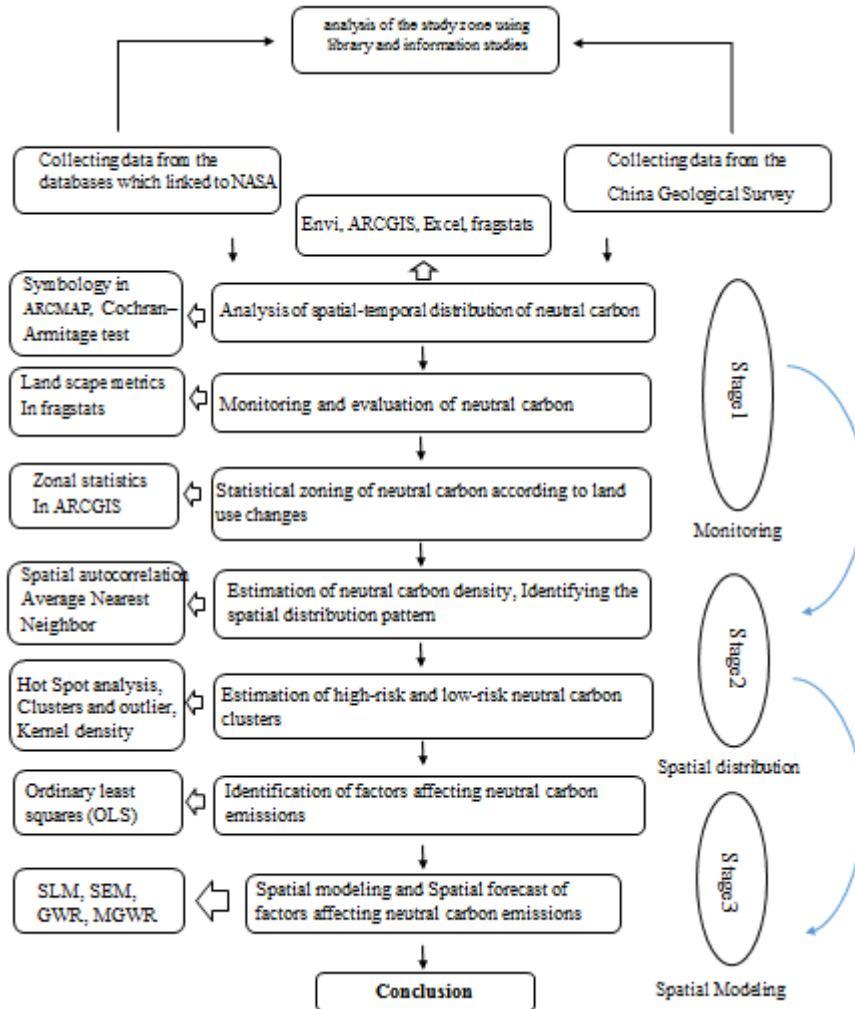


Figure. 2. Key Stages of the Current Study

2.2. Spatiotemporal analysis

To assess trends in the Carbon Storage, the Cochran–Armitage test was used to identify linear trends during the 30 years. This test was used to determine whether there were any significant changes in Carbon Storage over the study period (Nam, 1987).

A choropleth map, which uses a color range to show changes in the layers of polygons (Symbology), was produced at the township level during the study period.

2.3. Zonal Statistics

Calculates statistics on values of a raster within the zones of another dataset. A zone is defined as all input areas with the same value. The areas do not have to be contiguous. Both raster and feature can be used for the zone input.

When the cell size of the input raster or feature zone data and the input value raster are different, the output cell size will be the maximum of inputs, and the input value raster will be used as the snap raster internally. If the cell size is the same, but the cells are not aligned, the input value raster will be used internally as the snap raster. Either of these cases will trigger an internal resampling before the zonal operation is performed.

2.4. Landscape metrics

Landscape metrics are algorithms that quantify specific spatial characteristics of patches, classes of patches, or entire landscape mosaics. There are many quantitative measures of landscape composition, including the proportion of the landscape in each patch type, patch richness, patch evenness, and patch diversity. Software packages are widely used (e.g., FRAGSTATS, see [McGarigal & Marks, 1995](#); [McGarigal et al., 2002](#)), and many metrics have also been integrated into existing geographic information system (GIS) software (e.g., Patch Analyst in ArcMap; and module Pattern in IDRISI).

2.5. Point density

Point density' calculates the density of point features around each output raster cell. Conceptually, a neighborhood is defined around each raster cell center, and the number of points that fall within the neighborhood is totaled and divided by the area of the neighborhood (ArcGIS help 10.6.1).

2.6. Kernel density

Calculates a magnitude-per-unit area from a point or polyline features using a kernel function to fit a smoothly tapered surface to each point or polyline. Larger values of the search radius parameter produce a smoother, more generalized density raster. Smaller values produce a raster that shows more detail. Only the points or portions of a line that fall within the neighborhood are considered in calculating density. If no points or line sections fall within the neighborhood of a particular cell, that cell is assigned No Data ([Silverman, 1966](#)).

2.7. Average nearest neighbor

'Average nearest neighbor' measures the distance between each feature centroid and its nearest neighbor's centroid location. It then averages all of these nearest-neighbor distances. If the average distance is less than the average for a hypothetical random distribution, the distribution of the analyzed features is considered clustered. If the average distance exceeds a hypothetical random distribution, the features are considered dispersed. The pattern exhibits clustering if the average nearest neighbor ratio is less than 1. If the index is greater than 1, the trend is toward dispersion ([Mitchell, 2005](#)).

2.8. Spatial autocorrelation

Spatial correlation and autocorrelation play a significant role in spatial modeling. A wide variety of methods for testing and measuring spatial autocorrelation have been improved; many geographers are keen on utilizing Moran's I, which is one of the well-known spatial autocorrelations ([Bivand et al., 2011](#)). The global Moran's I index value is within a range of -1.0 to $+1.0$. This index which is a demonstrator of the spatial pattern, is defined as (> 0) clustered, ($= 0$) dispersed, and (< 0) for random distribution ([Bivand et al., 2011](#)). In the present study, the global Moran's I investigated the spatial distribution pattern of Carbon Storage for each feature. The global Moran's I index value must show the clustering distribution pattern to find high and low-risk clusters for further analysis.

2.9. Hot spot analysis

After obtaining the clustering pattern, the spots with the highest incidence, high-risk spots, were analyzed. The Getis-Ord G_i^* statistic was accordingly determined for features by the hot spot analysis (Getis-Ord G_i^*) tool in ArcGIS software. The Getis-Ord G_i^* statistic is calculated by comparing the local sum of the value for the feature in question and those of its neighbors to the sum of all feature values ([Kim et al., 2017](#)) Zscore was obtained from G_i^* statistic for positive Z-scores; the more significant Z-score reflects the more intensity of the clustering high values. For negative Z-scores, the smaller Z-score represents the more intense and the clustering of low values (i.e., a cold spot is obtained) ([Peeters et al., 2015](#)).

2.10. Anselin local Moran's I

Anselin local Moran's I was used to provide information on regions with high or low risks. This index divides polygons into five categories: high-high, low-low (indicating a clustering pattern), low-high, high-low (showing an outlier pattern), and insignificant. High-high (HH) reveals the areas that along with their surroundings, have a high Carbon Storage and, in turn, shows the high-risk clusters or hotspots. While low-low (LL) spots illustrate the areas in which the Carbon Storage is low and indicate the low-risk clusters of Carbon or cold spots ([Peeters et al., 2015](#)).

The next step was to explore Global and Local regression models that might better explain the variation in Carbon Storage based on the effective (Land cover, NDVI, LST) factors. Spatial autocorrelation (Global Moran's I) was utilized to assess whether the explanatory factors exhibited a random spatial pattern and where adequate models have a random distribution of the residuals.

2.11. Ordinary least squares (OLS)

The OLS is a regression method investigating the relationships between a set of explanatory or independent variables and a dependent variable. OLS uses two major implicit assumptions: the observations are independent and constant across the study area, and the error terms are not correlated ([Anselin & Arribas-Bel, 2013; Oshan et al., 2020](#)). OLS assumes that the observations at the county level are independent of each other and does not consider spatial dependence. SLM is denoted by:

$$y_i = \beta_i + x_i\beta + \varepsilon_i \quad (1)$$

This method minimized the sum of squared differences between the observed response and the ones predicted from the explanatory method. OLS regression is a powerful technique for modeling continuous data, mainly when it is used in conjunction with dummy variable coding and data transformation ([Boulos et al., 2001](#)). The Carbon Storage case was the dependent variable used in the model.

The least square regression model interpretation was based on multicollinearity, robust probability, adjusted R, and Akaike's information criteria. The robust probability indicates the statistically significant variables, which shows their significance in the model. In other to examine the VIF values and robust probability OLS model was run several times till all the redundant variables were removed from the model. This procedure continued until narrowing down to non-redundant and significant variables; Akaike's information criterion (AIC) was then used to determine the best OLS model.

In reality, however, and in the case of Carbon Storage, we know that variables are spatially correlated (as supported by the results of SEM and SLM later on). These interactions are omitted from OLS; therefore, OLS is a misspecified model in this case ([Anselin & Arribas-Bel, 2013](#)). Thus, we used SLM and SEM, both variants of OLS ([Anselin, 2003](#); [Ward & Gleditsch, 2018](#)), and took spatial dependence into account but modeled it differently.

2-12- Spatial lag model (SLM)

The SLM assumes dependency between the dependent variable and explanatory variables and incorporates spatial dependence into the regression model with a "spatially lagged dependent variable" ([Anselin, 2003](#); [Ward & Gleditsch, 2018](#)). SLM is denoted by:

$$y_i = \beta_0 + x_i\beta + \rho W_i y_i + \varepsilon_i \quad (2)$$

Where ρ is the spatial lag parameter (spatial autoregressive parameter), and W_i is a vector of spatial weights (a row of the spatial weights matrix). Eq. (2) is constructed by decomposing the error term in Eq. (1) ([Ward & Gleditsch, 2018](#)). The weight matrix (W) on the right-hand side of this equation specifies the neighbors at location i and, as such, relates the independent variable to the explanatory variables at that location ([Anselin & Arribas-Bel, 2013](#)). The presence of spatial lag suggests a potential diffusion process ([Kostov, 2010](#)).

2.13. Spatial error model (SEM)

The SEM assumes spatial dependence in the error term of OLS and decomposes the error term in Eq. (1) into two terms ($\lambda W_i \zeta_i$ and ε_i below) ([Anselin, 2003](#); [Chen et al., 2016](#)). The general form of this model is ([Ward & Gleditsch, 2018](#)):

$$y_i = \beta_0 + x_i\beta + \lambda W_i \zeta_i + \varepsilon_i \quad (3)$$

Where at county i , ζ_i indicates the spatial component of the error, λ indicates the level of correlation between these components, and ε_i is a spatially uncorrelated error term.

2.14. Local models

- **Geographically weighted regression (GWR)**

Global regression models such as OLS, SEM, and SLM implicitly assume spatial stationarity in the relationships between explanatory variables and dependent variable(s), meaning that they assume these relationships do not vary over space (Brunsdon et al., 1996; Brunsdon et al., 1998). To relax this assumption and to allow for “parameters to vary spatially.” Brunsdon et al. (1996) introduced GWR as an extension of general regression models based on kernel-weighted regression. Instead of estimating global values for regression parameters, GWR allows these parameters to be derived for each location separately, and in doing so, it incorporates geographic context (Oshan et al., 2020). GWR is denoted by (Fotheringham & Oshan, 2016):

$$y_i = \beta_0 + \sum_{j=1}^m \beta_j X_{ij} + \varepsilon_i, \quad i = 1, 2, \dots, n \quad (3)$$

Where at county i , y_i is the value for the Carbon Storage, β_0 is the intercept, β_j is the j^{th} regression parameter, X_{ij} is the value of the j^{th} explanatory parameter, and ε_i is a random error term. Parameter estimates for each explanatory variable.

The results were analyzed in the spatial relationship tools within the spatial statistics toolbox in the ArcGIS Arc toolbox. The explanatory variables used in OLS, SEM, and SLM were used in the GWR modeling to assess the difference in model improvement, which can be due to the modeling approach or effective factors. The GWR model was applied to analyze the relationship between Carbon Storage and effective factors (land cover, NDVI, LST) changes from one feature to another. The GWR detects spatial variation, shows how the relationship varies in space, produces valuable information for interpreting spatial nonstationarity (Vandenbroucke et al., 2012).

- **Multiscale GWR (MGWR)**

Even though GWR can be a significant improvement compared to global regression in the context of spatial processes, it still assumes that the scale of all of the involved relationships is constant over space and thus does not allow for analyzing these relationships at different scales (Fotheringham et al., 2017; Oshan et al., 2019).

In many cases, including Carbon Storage, this assumption is invalid because different processes are involved with varying spatial scales. MGWR is an extension of GWR that allows studying the relationships at varying spatial scales and achieves that by using varying bandwidth as opposed to a single, constant bandwidth for the entire study area (Fotheringham et al., 2017; Yu et al., 2019). MGWR can be formulated as (Fotheringham et al., 2017):

$$y_i = \sum_{j=0}^m \beta_j X_{ij} + \varepsilon_i, \quad i = 1, 2, \dots, n \quad (5)$$

Where β_j is the bandwidth used to calibrate the j^{th} relationship (Fotheringham et al., 2017), the rest of the parameters are the same as Eq. (1).

3. EXPERIMENTAL RESULTS

This section consisted of four phases. In the first phase distribution of CO₂ over the Hunan province is analyzed. In the second phase average of the 15 years of CO₂ monitoring over Hunan province is analyzed, and high-risk and low-risk areas are identified. In the third phase relationship between three environmental parameters and CO₂ is analyzed over Hunan province. The last phase tries to simulate the future trend of CO₂ over the Hunan province using statistical methods.

3.1. Phase 1

In this study, after collecting information from the giovanni.gsfc.nasa.gov website, ARCGIS PRO software was used to perform a spatiotemporal analysis of CO₂ from 2002 to 2017. The complete specification of CO₂ used in this study is reported in Table 2.

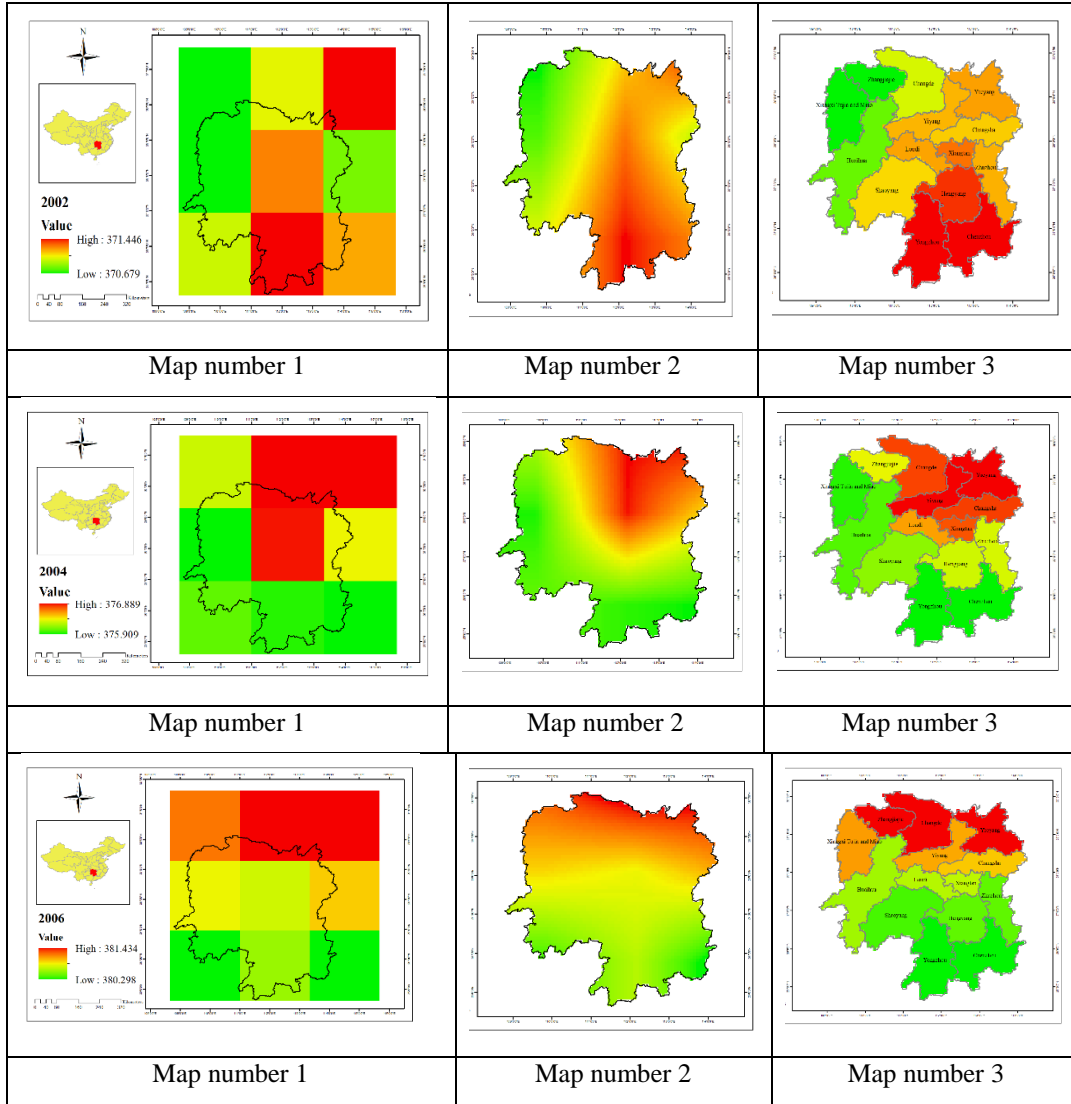
Table 2. CO₂ products from 2002 to 2017

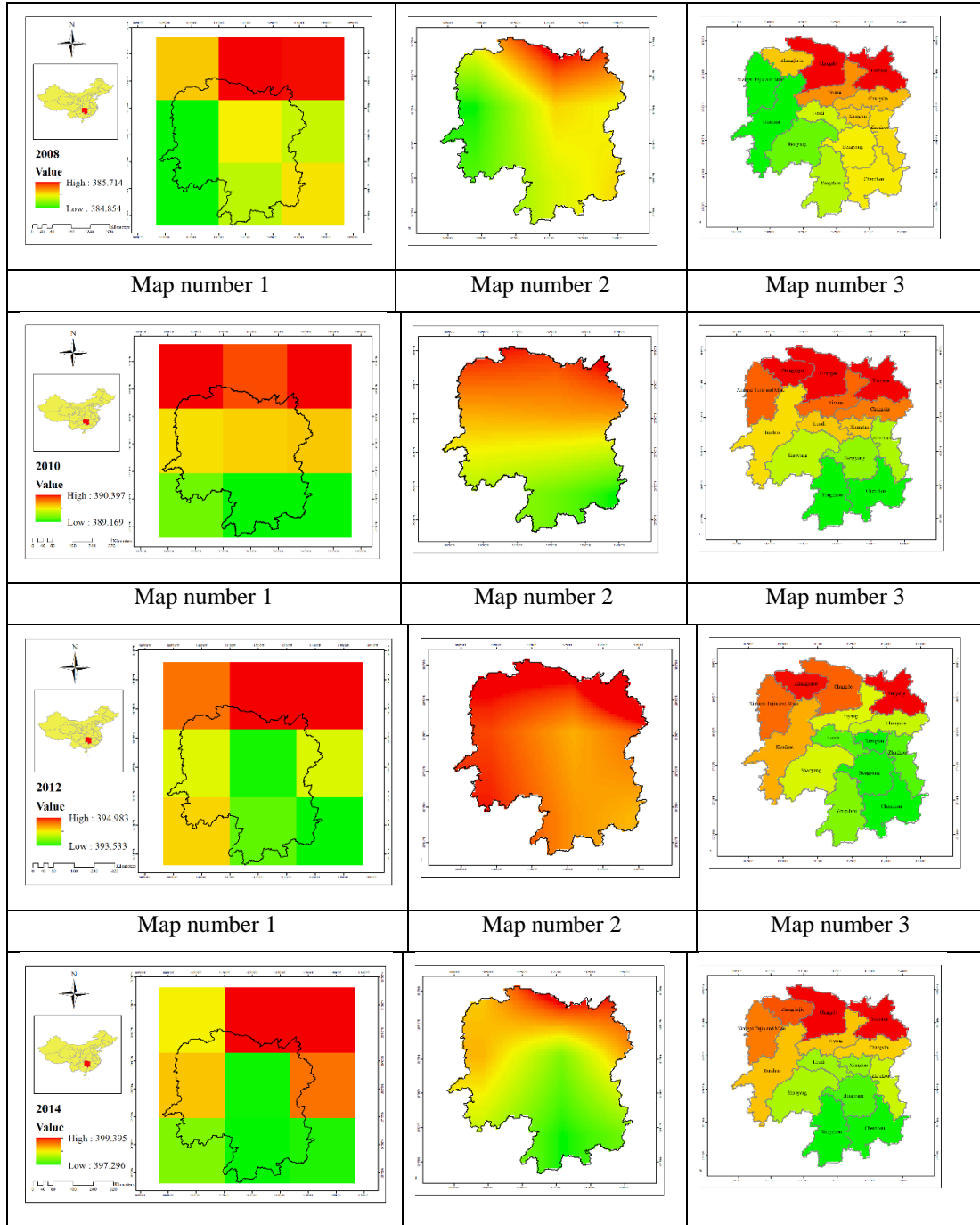
Variable	Units	Source	Temp.res.	Spat.res. (degrees)	Begin date	End date
CO ₂	PPM	AIRS	Monthly	2*2.5	2002	2017

In the first step, a map output for 15 years (from 2002 to 2017) was taken from the primary CO₂ product without changing the cell size, corresponding to map number 1. In the second step, to improve the color tonality and CO₂ changes in Hunan province, the cell size was enhanced by 0.08 degrees, which was done with the Resample tool. The output of this work is map number 2. In the last step of this section, which is related to map number 3, using the Zonal statistics tool in the spatial analysis toolbox, the average pixel values (CO₂) were calculated by the cities of Hunan province (Figure 3).

The Resample function changes the raster pixel size, the resampling type, or both. Before combining and analyzing rasters with different resolutions and map projections, it is often desirable to resample the data to a common resolution and projection.

A zonal statistics operation calculates statistics on cell values of a raster (a value raster) within the zones defined by another dataset. The Zonal Statistics tool calculates only one statistic at a time and creates a raster output. This value becomes the cell value of the raster output for the cells corresponding to that zone. If a zone feature contains overlapping zones, the statistic is computed for only one zone because a cell in the output raster can represent only one value.





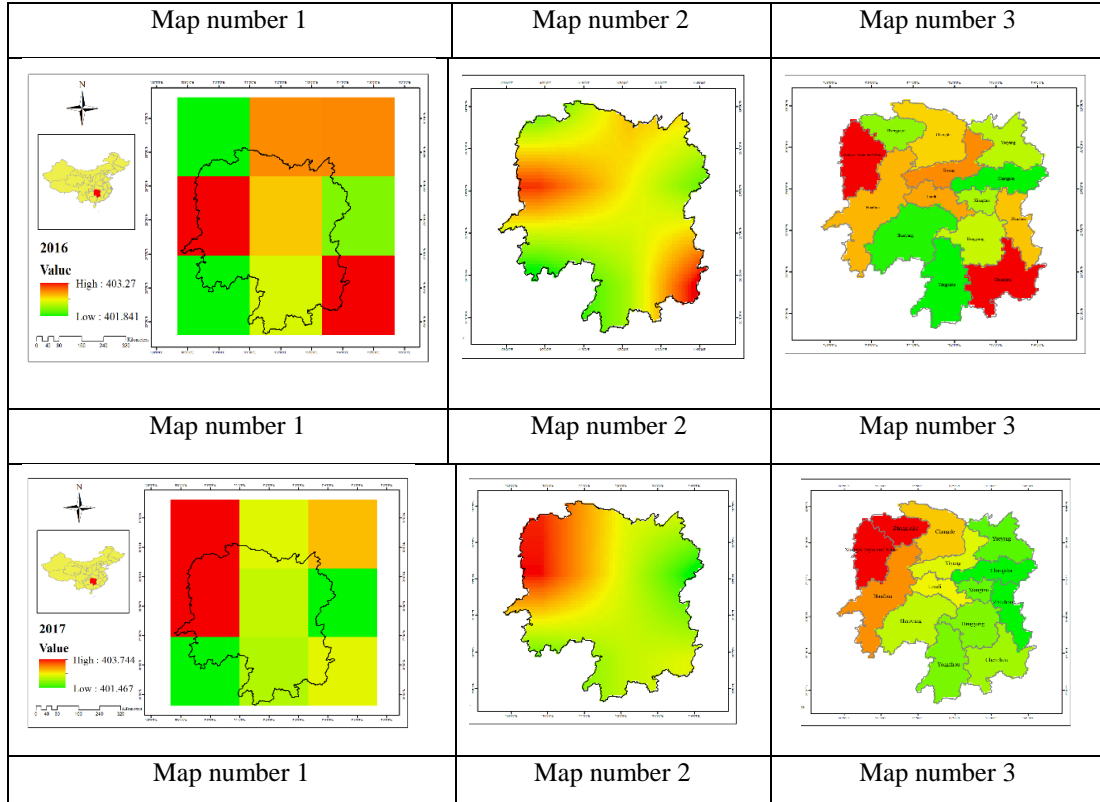


Figure 3. Distribution of CO₂ over the Hunan from 2002 to 2017 with lag size 2 in year. Map number 1 is the primary CO₂ product. Map number 2 is an enhanced CO₂ product with the Rsample tool. Map number 3 is the results of Zonal statistics.

3.2. Phase 2

The next step calculates the 15-year average of carbon dioxide emissions from 2002 to 2017. In the average map, the northern regions of Hunan Province showed a high rate of CO₂ (Figure 4). A 15-year average map was used to identify high-risk and low-risk clusters of CO₂ at the scale of cities in Hunan province, China. At this stage, it is necessary first to identify the pattern of spatial distribution in the form of clusters. For this reason, the local Moran test (spatial autocorrelation) was used in the first step. As a result of this test, Moran's Index is above zero (Moran's Index = 0.520) and Z-score = 6.983, which shows the clustering of the CO₂ distribution pattern at the border of the study. This result is statistically significant (P_value=0), and there is less than one percent chance that this pattern is randomly identified (Figures 4 and 5).

After confirming the results of this test (clustering of the CO₂ distribution pattern), high-risk and low-risk CO₂ clusters can be determined locally (city by city). For this purpose, the local Moran's test was used, which included hot spot and cold spot analysis and Clusters and outliers analysis. Figure (6) shows that in hotspot analysis, high-risk

clusters were identified in northern cities and low-risk clusters in southern cities. Most of the clusters are with a confidence level of 99%. Cluster and non-cluster analysis also showed the same results; no non-cluster was found (Figure 7). The results of this study showed that the two analyses of hotspots and cluster and non-cluster could be an excellent supplement to identify high-risk and low-risk clusters, which can be used in other studies.

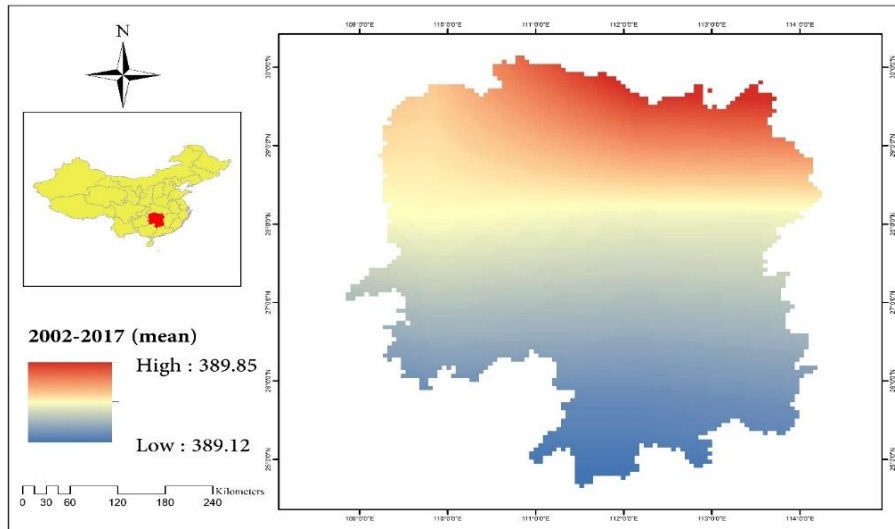


Figure 4. 15-year map of CO₂ emissions in Hunan province

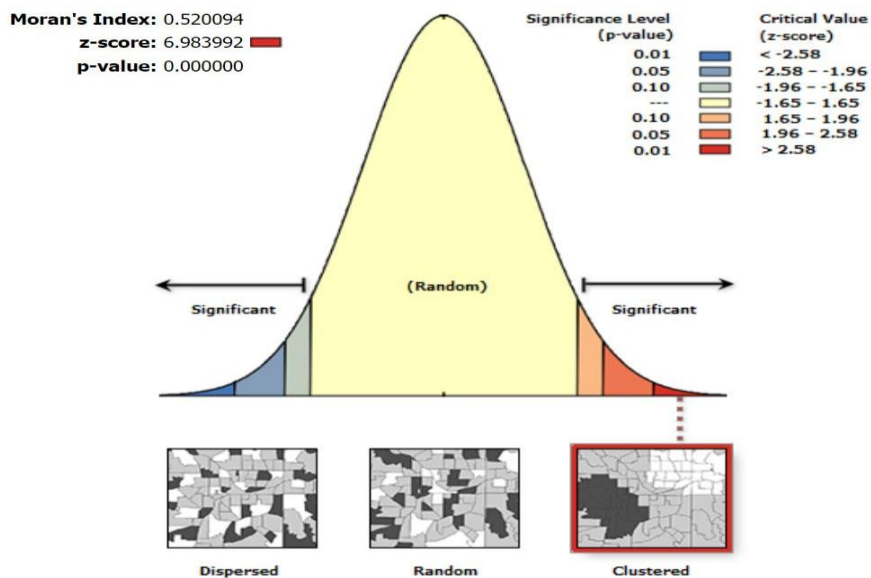


Figure 5. Moran's spatial autocorrelation test

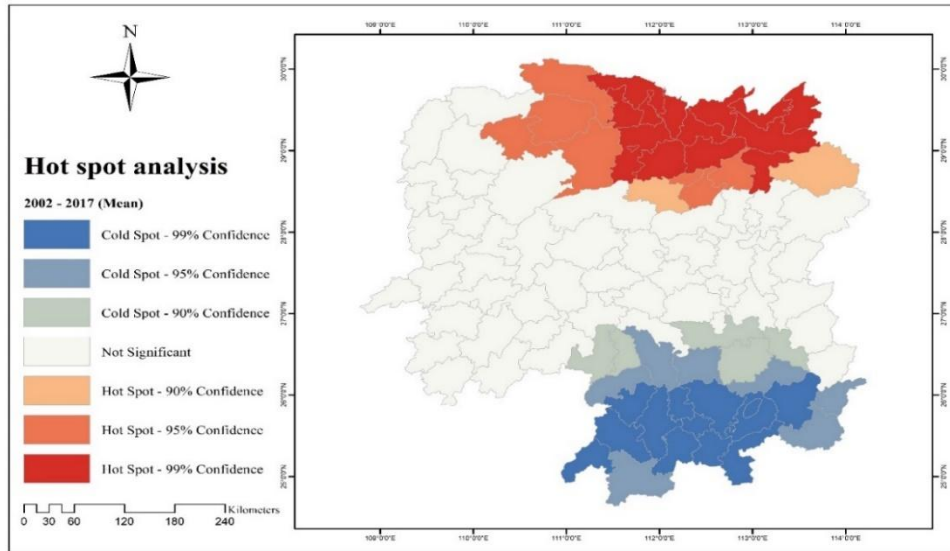


Figure 6. Hot spot analysis to identify high-risk and low-risk clusters

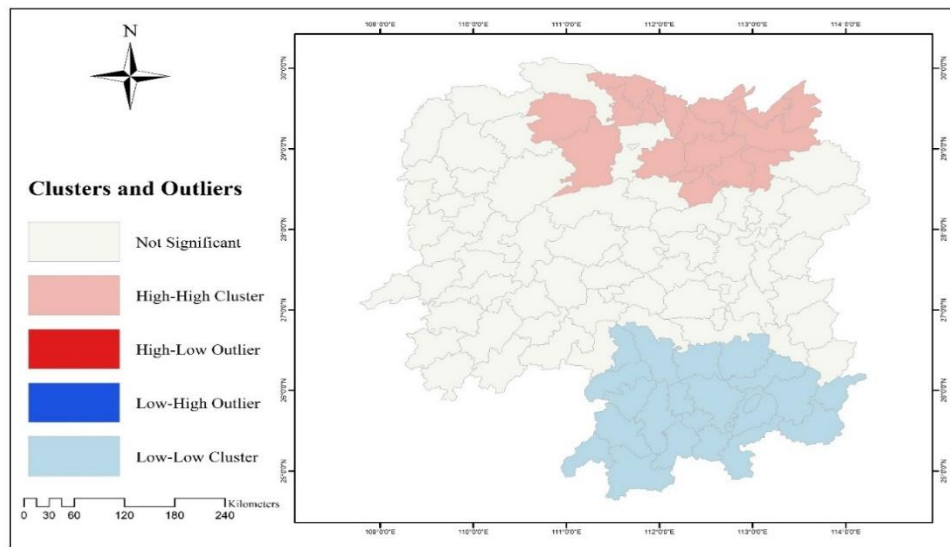


Figure 7. Cluster and non-cluster analysis to identify high-risk and low-risk clusters

3.3. Phase 3

Table 3 examines the relationship between three variables of land surface temperature, vegetation index, and land cover individually with the carbon dioxide variable. After inserting the dependent and independent variables in the ordinary least squares regression, the results showed that all three independent variables, LST, NDVI, and Land cover, are influential variables on carbon dioxide in Hunan Province, China (and Robust_Pr <0.03 (Probability))

Table 3. The relationship of each variable with CO₂ by ordinary least squares regression

Variable	Coefficient [a]	StdError	t-Statistic	Probability [b]	Robust_SE	Robust_t	Robust_Pr [b]
LST	0.084935	0.014056	6.042468	0.000055*	0.017307	4.907430	0.000362*
NDVI	-0.829229	0.157826	-5.254082	0.000202*	0.093134	-8.903652	0.000430*
Land cover	0.187599	0.027118	6.918007	0.000013*	0.020151	9.309602	0.000000*

The earth temperature variable with a coefficient of 0.084935 is directly related to carbon dioxide. However, the intensity of this relationship is less than the other two variables. Also, in the land use variable, the amount of CO₂ increases with decreasing density of green lands and increasing construction areas. In other words, the relationship between the two variables, Landcover, and CO₂, is direct (Coefficient = 0.187599). However, the vegetation variable is inversely related to carbon dioxide (Coefficient = -0.829229). The intensity of this relationship is more than the other two variables. It can be inferred that this index is more effective than other variables; all three variables had a statistically significant relationship with the CO₂ variable.

After identifying the influencing variables on CO₂, the identified variables were modeled in order to predict CO₂ for 2030. For this purpose, the relationship between the influencing variables of LST, NDVI, and Land Cover was investigated as a group with the CO₂ variable. After various tests and errors, LST and NDVI variables were finally modeled together by OLS, which had a significant relationship with CO₂ (Table 4).

Table 4. Investigating the relationship between LST and NDVI variables with CO₂ by ordinary least squares regression

Variable	Coefficient [a]	StdError	t-Statistic	Probability [b]	Robust_ SE	Robust t_ [b]	Robust_Pr [b]	VIF [c]
Intercept	186.275975	43.8094	4.251962	0.001368*	31.14035	5.981821	0.000085*	-----
LST	0.709363	0.14289	4.964246	0.000425*	0.101736	6.972586	0.000018*	7.8565
NDVI	-5.163193	1.30178	-3.96626	0.002219*	0.908947	-5.68041	0.000136*	7.8565

Also, to verify this model's applicability in predicting CO₂ for 2030, other statistics were checked, including AIC, which was at the lowest possible value, and R², whose value was above 0.8, which indicates a high percentage of confidence. The model created is in predicting CO₂. Also, Koenker's statistic (BP) is not statistically significant, showing the developed model's stability and consistency (Table 5).

Table 5. Examining the applicability of the model for predicting CO₂ in 2030

Akaike's Information Criterion (AICc)	Adjusted R-Squared	Koenker (BP) Statistic
26.793421	0.788944	0.752355

Also, this study found that GWR creates a more consistent and stable model than OLS, which is why GWR regression was used to predict the model (Table 6).

Table 6. Comparing the efficiency of the GWR model compared to OLS

Regressions	Akaike's Information Criterion (AICc)	Adjusted R-Squared
OLS	26.793421	0.858944
GWR	21.675436	0.9158433

After ensuring the model was created according to these independent variables, and calculating their amount in 2030 using the products of 2000 and 2010, the amount of CO₂ was calculated using GWR regression for the future (Figures 8 and 9).

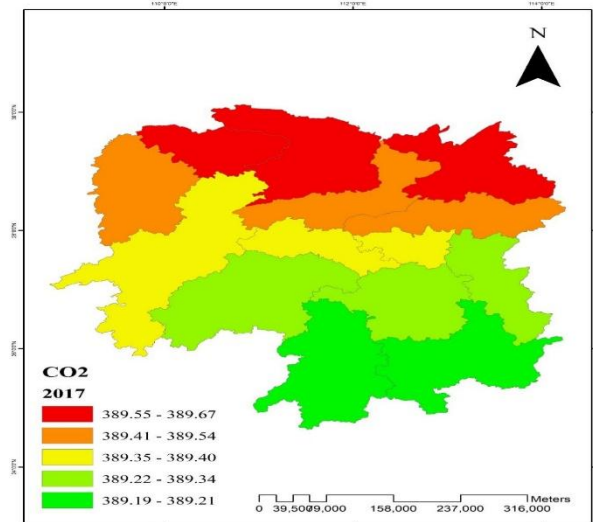


Figure 8. CO₂ calculated in 2017

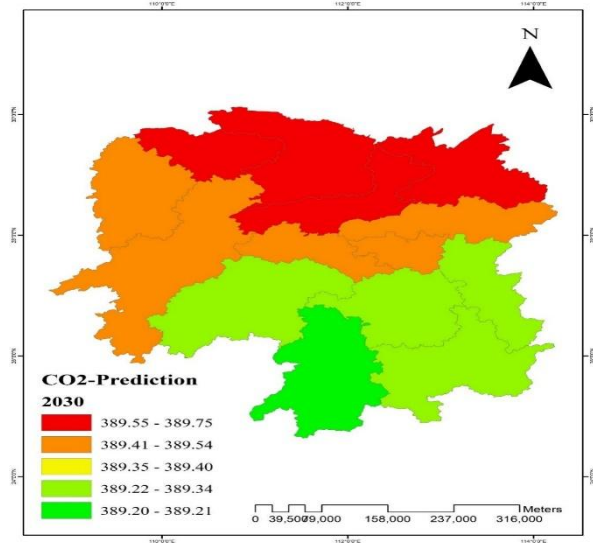


Figure 9. Predicted CO₂ with GWR in 2030

4. CONCLUSIONS

This study emphasizes Hunan province's vital role in combating climate change through effective carbon management, using remote sensing and spatial statistical methods to identify high-risk and low-risk emission clusters. Our analysis reveals important socio-economic and energy drivers of CO₂ emissions and provides important insights into the dynamics of this industrial region. The developed forecast model predicts carbon emission

trends for the next decade, emphasizing the need for targeted mitigation strategies, especially after temporary reductions during the COVID-19 pandemic. By providing a replicable framework for emissions monitoring and management, this research not only supports local policymakers but also highlights the importance of data-driven approaches in addressing broader emissions challenges in China and beyond.

ACKNOWLEDGEMENT

This research was supported by Xinjiang Institute of Ecology and Geography, Chinese Academy of Sciences, Urumqi 830011, China, Tianchi Talents Project of Xinjiang (E3350107); National Natural Science Foundation of China (No.42107084); Key Research and Development Program of Xinjiang (2022B01032-4). Professor YU Ruide is also given special gratitude that provided insight, support and expertise that greatly assisted the research.

LITERATURE

- Anselin, L., 2003. Spatial externalities, spatial multipliers and spatial econometrics. *Int. Reg. Sci. Rev.* 26 (2), 153–166.
- Anselin, L., Arribas-Bel, D., 2013. Spatial fixed effects and spatial dependence in a single cross-section. *Pap. Reg. Sci.* 92 (1), 3–17.
- Bivand R, Anselin L, Berke O, Bernat A, Carvalho M, Chun Y, Dormann C, Dray S, Halbersma R, Lewin-Koh N: spdep: Spatial dependence: weighting schemes, statistics and models. In: R package version 0.5–31, URL <http://CRAN.R-project.org/package=spdep>; 2011.
- Boulos MK, Roudsari AV, Carson ER. Health geomatics: an enabling suite of technologies in health and healthcare. *J Biomed Inform.* 2001;34(3):195–219.
- The British Petroleum (BP) Company, 2016. BP Statistical Review 2016. China's energy market in 2015. <http://www.bp.com/content/dam/bp/pdf/energy-economics/statistical-review-2016/bp-statistical-review-of-world-energy-2016-china-insights.pdf>.
- Brunsdon, C., Fotheringham, A.S., Charlton, M.E., 1996. Geographically weighted regression: a method for exploring spatial nonstationarity. *Geogr. Anal.* 28 (4), 281–298.
- Brunsdon, C., Fotheringham, S., Charlton, M., 1998. Geographically weighted regression. *Journal of the Royal Statistical Society: Series D (The Statistician)* 47 (3), 431–443
- Chen, Y., Chang, K.T., Han, F., Karacsonyi, D., Qian, Q., 2016. Investigating urbanization and its spatial determinants in the central districts of Guangzhou, China. *Habitat International* 51, 59–69.
- Flannigan et al., 2005. M.D. Flannigan, B.D. Amiro, K.A. Logan, B.J. Stocks, B.M. Wotton Forest fires and climate change in the 21ST century Mitig. Adapt. Strat. Glob. Change, 11, 847-859
- Fotheringham, A.S., Oshan, T.M., 2016. Geographically weighted regression and multicollinearity: dispelling the myth. *J. Geogr. Syst.* 18 (4), 303–329
- Fotheringham, A.S., Yang, W., Kang, W., 2017. Multiscale geographically weighted regression (MGWR). *Annals of the American Association of Geographers* 107 (6), 1247–1265.

- Kim S-M, Choi Y. Assessing statistically significant heavy-metal concentrations in abandoned mine areas via hot spot analysis of portable XRF data. *Int J Environ Res Public Health*. 2017;14(6):654.
- Kostov, P., 2010. Model boosting for spatial weighting matrix selection in spatial lag models. *Environment and Planning B: Planning and Design* 37 (3), 533–549.
- Liu, M., Wang, H., Wang, H., Oda, T., Zhao, Y., Yang, X., Zang, R., Zang, B., Bi, J., Chen, J., 2013. Refined estimate of China's CO₂ emissions in spatiotemporal distributions. *Atmospheric Chemistry and Physics* 13,10873-10872.
- Liu, Z., Guan, D., Scott, M., Henry, L., Z., L., Jun, S., Zhang, Q., D., G., 2015. Steps to China's carbon peak. *Nature* 522, 279-281.
- Liu, Z., Guan, D., Wei, W., Davis, S.J., Ciais, P., Bai, J., Peng, S., Zhang, Q., Hubacek, K., Marland, G., Andres, R.J., Crawford-Brown, D., Lin, J., Zhao, H., Hong, C., Boden, T.A., Feng, K., Peters, G.P., Xi, F., Liu, J., Li, Y., Zhao, Y., Zeng, N., He, K., 2015. Reduced carbon emission estimates from fossil fuel combustion and cement production in China. *Nature* 524, 335-338.
- McGarigal, K., Cushman, S.A., Neel, M.C., Ene, E. (2002), "FRAGSTATS: Spatial Pattern Analysis Program for Categorical Maps", project homepage, University of Massachusetts, Amherst.
- McGarigal, K., Marks, B.J. (1995), "FRAGSTATS: Spatial Pattern Analysis Program for Quantifying Landscape Structure", General Technical Reports, PNW-GTR-351, Portland (USDA Forest Service, Pacific Northwest Research Station).
- Metsaranta, J.M.; Hudson, B.; Smyth, C.; Fellows, M.; Kurz, W.A. 2023. Future Fire Risk and the Greenhouse Gas Mitigation Potential of Forest Rehabilitation in British Columbia, Canada. *For. Ecol. Manag.* 529, 120729
- Mi, Z., Wei, Y.-M., Wang, B., Meng, J., Liu, Z., Shan, Y., Liu, J., Guan, D., 2017. Socio economic impact assessment of China's CO₂ emissions peak prior to 2030. *Journal of Cleaner Production* 142, 654 Part 4, 2227-2236.
- Mitchell, A. 2005. "The ESRI guide to GIS analysis: Vol. 2. Spatial measurement and statistics 2005 Redlands." In.: CA ESRI Press.
- Nam J-M. A simple approximation for calculating sample sizes for detecting linear trend in proportions. *Biometrics* 1987;701–5.
- Nguyen, A.T., 2019. Carbon Dioxide Emissions and Implications for Environmental Policy: Evidence in Southeast Asia. *Journal of Asian Energy Studies*, 3(1), pp.8-24.
- Oshan, T.M., Smith, J.P., Fotheringham, A.S., 2020. Targeting the spatial context of obesity determinants via multiscale geographically weighted regression. *Int. J. Health Geogr.* 19 (1), 1–17.
- Peeters A, Zude M, Käthner J, Ünlü M, Kanber R, Hetzroni A, *et al.* Getis–Ord’s hot-and cold-spot statistics as a basis for multivariate spatial clustering of orchard tree data. *Comput Electron Agric.* 2015;111:140–50.
- Silverman, B. W. *Density Estimation for Statistics and Data Analysis*. New York: Chapman and Hall, 1986.
- Vandenbroucke JP, Pearce N. Incidence rates in dynamic populations. *Int J Epidemiol.* 2012;41(5):147.
- Wang, A., Lin, B., 2017. Assessing CO₂ emissions in China’s commercial sector: Determinants and reduction strategies. *Journal of Cleaner Production* 164, 1542-1552.
- Wang, H., Zhang, R., Liu, M., Bi, J., 2012. The carbon emissions of Chinese cities. *Atmospheric Chemistry and Physics* 12, 6197-6206.

- Ward, M.D., Gleditsch, K.S., 2018. Spatial regression models. 155. Sage Publications.
- World Trade Organization. (2007). International trade statistics 2007. Geneva. Xinhua. (2007). Official: Single-child parents in China can have second child Xinhua Journal, July 10, 2007.
- Xinhua, 2015. Enhanced actions on climate change: China's intended nationally determined contributions http://news.xinhuanet.com/2015-06/30/c_1115774759.htm.
- Yu, H., Fotheringham, A.S., Li, Z., Oshan, T., Kang, W., Wolf, L.J., 2019. Inference in multiscale geographically weighted regression. *Geogr. Anal.* 52, 87–106.

MAGAZYNOWANIE WĘGLA W PROWINCJI HUNAN: MONITOROWANIE, MODELOWANIE I STRATEGIE ZARZĄDZANIA W CELU ŁAGODZENIA ZMIAN KLIMATYCZNYCH

SŁOWA KLUCZOWE: przechowywanie węgla, monitorowanie, modelowanie, dane uzyskane zdalnie, prowincja Hunan

Streszczenie

Zmiana klimatu spowodowana przez emisję gazów cieplarnianych, zwłaszcza dwutlenku węgla (CO₂), jest jednym z najważniejszych wyzwań środowiskowych, z którymi świat mierzy się obecnie. Zrozumienie dynamiki przestrzennej i czasowej emisji CO₂ ma kluczowe znaczenie dla opracowania skutecznych strategii mitygacyjnych. W niniejszym badaniu zbadano profil emisji dwutlenku węgla w prowincji Hunan, ważnym regionie przemysłowym i ekonomicznym w południowych Chinach. Wykorzystując technologię teledetekcji, statystyki przestrzenne i modelowanie szeregów czasowych, naukowcy zidentyfikowali klastry emisji dwutlenku węgla wysokiego i niskiego ryzyka w prowincji Hunan. Ponadto w badaniu zbadano kluczowe czynniki społeczno-ekonomiczne i energetyczne, które napędzają emisję dwutlenku węgla. Na koniec autorzy opracowali model prognozowania, aby przewidzieć ślad emisji dwutlenku węgla w ciągu następnej dekady. Wyniki pokazują siłę integracji metod statystycznych i prognozowania geograficznego w celu zapewnienia opartych na dowodach spostrzeżeń wspierających politykę zarządzania emisją dwutlenku węgla na poziomie prowincji. Tę wieloaspektową metodologię można powtórzyć w innych regionach w celu wzmocnienia monitorowania gazów cieplarnianych i planowania redukcji emisji na skalę krajową. Wyniki te podkreślają kluczową rolę, jaką odgrywają chińskie prowincje w rozwiązywaniu globalnego kryzysu klimatycznego poprzez ukierunkowane działania łagodzące oparte na danych.

Details of authors:

Mr. Seyed Omid Reza Shobairi
e-mail: Omidshobeyri214@gmail.com

Dr. Sun Lingxiao
e-mail: sunlx@ms.xjb.ac.cn

Submitted 12.08.2024
Accepted 1.11.2024

